International Journal of ChemTech Research
CODEN (USA): IJCRGG ISSN : 0974-4290
Vol.6, No.11, pp 4643-4649, Oct-Nov 2014

Effect of doping and annealing on the room temperature magnetic and dielectric properties of La modified $BiFeO_3$ multiferroic nanoparticles synthesized by sol-gel citrate combustion method

A.Sathiya Priya and I. B. Shameem Banu*

Department of Physics, B S Abdur Rahman University, Vandalur, Chennai, India

***Corres.author: shameembanu@bsauniv.ac.in**

Abstract: We have investigated the effect of doping and annealing on the magnetic and dielectric properties of La doped $BiFeO_3$ multiferroic materials. The nanoparticles of the doped samples ($Bi_{1-x}La_xFeO_3$) were prepared by sol-gel citrate combustion method and were annealed at two different temperatures of 600 °C and 800 °C. The undoped $BiFeO_3$ was synthesized and calcined at 600 °C. XRD patterns reveal that $BiFeO_3$ and $Bi_{1-x}La_xFeO_3$ successfully crystallize in rhombohedral structure with R3c space group with no other secondary phase. La doping significantly enhanced the magnetic properties of undoped BiFeO3. The $Bi_{1-x}La_xFeO_3$ calcined at 600 °C exhibits the conspicuous room temperature magnetic hysteresis loop with high saturation whereas that calcined at 800 °C resulted in a low saturation magnetization. The samples annealed at different temperature show significant difference in their magnetic parameters such as remnant magnetization (M_r), saturation magnetization (M_s) and coercive field (H_c).The crystallite sizes also vary remarkably with calcination temperature and hence, it is inferred that crystallite size plays a vital role on the magnetic and dielectric properties of these two samples. Conductivity measurement signifies a better resistivity for low calcined sample.

Key words: Multiferroic, doped $BiFeO_3$; sol-gel method; annealing; ferromagnetism ; dielectric property

1. Introduction

Multiferroic materials show simultaneous ferroelectric and ferromagnetic ordering [1-4]. Owing to the coupling between ferroelectric and magnetic domains, multiferroism is likely to offer a whole range of new applications. Among the single-phase multiferroic materials, perovskite structured $BiFeO_3$ has potential applications in information storage, sensors and actuators. $BiFeO_3$ (BFO) has a rhombohedral R3c crystallographic structure with no inversion center and shows a spin-modulated cycloidal magnetic structure with a modulation period of ~62 nm. $BiFeO_3$ simultaneously shows antiferromagnetic and ferroelectric order with high transition temperatures (5-7), i.e. T_N~370°C and T_C~850°C, respectively. So, $BiFeO_3$ material gained substantial interest as it reveals magnetoelectric coupling at room temperature. However, superimposed incommensurate cycloid spin structure cancels out its macroscopic magnetization (8-10) and so it exhibits weak antiferromagnetism at room temperature and shows spatially non-uniform magnetic structure. To suppress the spiral spin structure and to enhance the magnetic moment, one of the effective method is to dope BFO. Other limitations of BFO are low electrical resistivity and large leakage current, which affect the ferroelectric properties and dielectric properties. These problems are due to the multiple oxidation states of Fe ion, Fe^{3+} and Fe^{2+} and this causes the electron hopping from Fe^{2+} to Fe^{3+}at high electric filed (10, 11). The oxygen vacancies are are created due to the highly volatile nature of BFO. Cationic substitution at Bi site proved to be effective in controlling the leakage current and oxygen vacancies in improving the dielectric properties (6, 7, 12).

Doping of rare earth ions such as La^{3+}, Sm^{3+} and Nd^{3+} (13-16) to BFO at Bi site has enhanced the electrical and magnetic properties of BFO. The electrical and magnetic properties also depend on the growth parameters as Bi is volatile. The calcination (annealing) temperature which is also one of the important parameter during the growth process has impact on the crystallite size and consequently exhibits interesting results of magnetic and dielectric properties [17, 18]. Hence, taking into consideration of the doping and annealing effect, in this report, La doped BFO, $Bi_{1-x}La_xFeO_3$ (x = 1%) nanoparticles were prepared by the sol-gel citrate combustion method and calcined at two temperatures 600° C and 800° C to investigate effect on the magnetic and dielectric property of the samples. To illustrate the results of $Bi_{1-x}La_xFeO_3$ (BLFO) relatively, BFO was also prepared at calcination temperature of 600° C and its magnetic and dielectric property were also measured.

2. Experimental details

$BiFeO_3$ and $Bi_{1-x}La_xFeO_3$ (x = 1%) nanoparticles were synthesized by sol-gel citrate combustion method (Fig. 1). Analytical grade bismuth (III) nitrate pentahydrate (assay 98% Merck), ferric nitrate (assay 98% Merck), lanthanum (III) nitrate hexahydrate (assay 99.9% Alfa Aesar), citric acid anhydrous (assay 99.5% Merck) and nitric acid (assay 70% Merck) were used as starting materials. Double distilled water was used to prepare experimental solutions. All the chemicals used were of analytical reagent grades, which do not require further purification. The double distilled water was used as solvents for all the solutions prepared. Stoichiometric amounts of the required starting materials were dissolved in dilute nitric acid and double distilled water. Citric acid was added in 1:1 molar ratio with metal nitrates with constant string at 90°C for 6 h. At the end of combustion, brownish powder is formed. Finally, the obtained BLFO powders were calcined at 600°C and 800°C for 4 h and BFO was calcined at 600°C.

The phase identification was performed for all prepared nanoparticles by X-ray diffractometer with an X Pert Pro X- ray diffractometer (PANalytical) with Cu K_α radiation of wavelength 1.5404 Å at the scanning rate 0.02 min^{-1} in the range of 2θ being 10° to 90°. The magnetization hysteresis (M-H) loop were obtained at room temperature using vibrating sample magnetometer (EG&G PARC VSM 155). Dielectric properties were measured using LCR dielectric spectrometer (HIOKI 3532-50 LCR HITESTER) at room temperature in the frequency range from 100 Hz to 10 MHz.

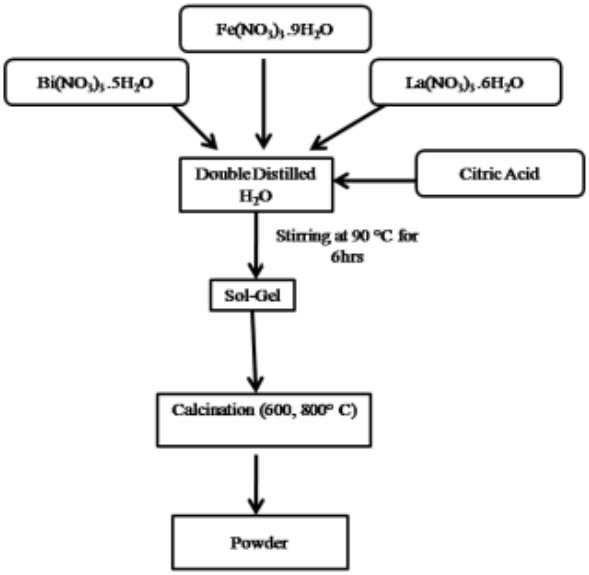

Fig. 1. Flow chart of sol-gel method

3. Results and discussions

3.1. Structural analysis

Fig. 2 shows the XRD pattern of the prepared nanoparticles. BFO synthesized at room temperature is found to be amorphous in nature as shown by the XRD in which the peaks in the 2θ range from 10° to 90° are absent. For the undoped BFO, an impurity peak corresponding to $Bi_2Fe_4O_9$ appears at 30° in the 2θ range and

this impurity peak disappears for the 600°C and 800°C calcined BLFO confirming the formation of pure rhombohedral phase after doping. The broad diffraction peaks indicate that the size of the crystallites is in the nanometer scale. All the XRD peaks for BFO and BLFO coincide with that of standard $BiFeO_3$ diffraction pattern which correspond to perovskite based rhombohedral structure (JCPDS data card no - 86-1518). It can be seen that the addition of La does not affect the rhombohedral structure of $BiFeO_3$ [19] and in fact it has eliminated the impurity phase found for undoped BFO. Besides, a small shift of the peaks in the lower angle is observed for BLFO relative to BFO. This observation indicates that La^{3+} ions has replaced the Bi^{3+} ions effectively with small increase in the lattice parameters as the ionic radius of La^{3+} ions is greater than Bi^{3+} ions, but without significantly distorting the lattice of BFO. Improved crystallinity is observed for BLFO (600°C) as compared to BLFO (800°C). The average particle size was determined from the diffraction line width based on Scherrer's formula.

$$d=\frac{0.9\lambda}{\beta\cos\theta}$$

where, θ is the Bragg's angle, β is the Full width at half maximum and λ =1.54056 Å. The average crystallite size of BFO, BLFO (600°C) and BLFO (800°C) are 31, 56 and 93 nm respectively.

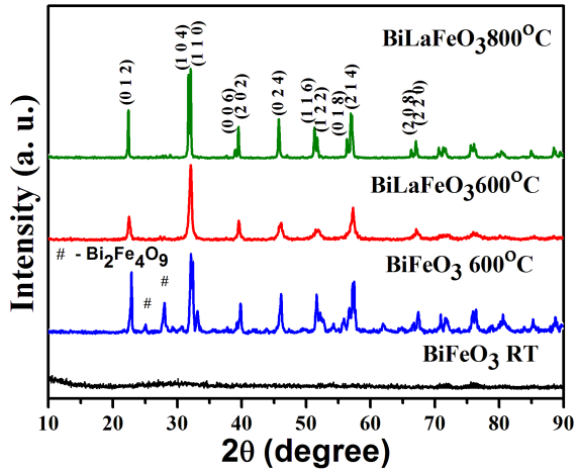

Fig. 2. Powder X-Ray Diffraction pattern of the undoped and doped BFO

3.2. Magnetic property

Table. 1. Room temperature saturation magnetization (M_s), remnant magnetization (M_r), coercivity (H_C) and magnetic susceptibility (χ) for BFO and BLFO.

Sample	M_s emu/g	M_r emu/g	H_C Oe	χ (emu g^{-1} Oe^{-1})
BFO	0.27	0.02	124	0.09 x 10^{-3}
BLFO (600°C)	1.60	0.12	97	0.13 x 10^{-3}
BLFO (800°C)	0.38	0.06	195	0.22 x 10^{-3}

The room temperature magnetic hysteresis curves (M-H curve) measured for the maximum applied field of ±10 kOe for BFO, BLFO (600°C) and BLFO (800°C) are shown in Fig. 3. Table 1 presents the remnant magnetization (M_r), saturation magnetization (M_s) and coercive field (H_c) values of the prepared samples. A very weak ferromagnetism is observed for BFO nanoparticles [20] in contrast to its bulk counterpart [21, 22]. It is known that in pure bulk BFO, the net magnetization is cancelled due to space modulated spin cycloidal structure. The exhibited weak magnetization of undoped BFO is due to the BFO nanoparticles. This can be understood from the fact that the increased surface to volume ratio at nanoscale interrupts the long-range antiferromagnetic order at the surfaces causing the surface-induced weak ferromagnetism.

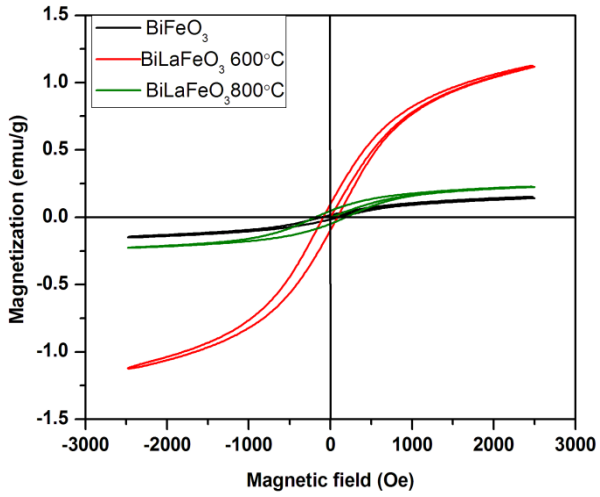

Fig.3. Room temperature magnetic hysteresis (M-H) curves

When La is doped to BFO, it is seen that magnetization has enhanced compared to undoped BFO. The enhancement is due to the suppression of the cycloidal spin structure of BFO when La is doped [23]. Ionic radius of La^{3+} is greater than ionic radius of Bi^{3+} (≈ 0.014 nm) and so strain introduced in the lattice due to large ion substitution would have also induced magnetization. Conspicuous well saturated magnetic hysteresis loop is obtained for BLFO (600°C) compared to BLFO (800°C). This difference is mainly considered to be due to the difference in the strain induced in the lattice during doping process. The strain is useful in canting of the Fe moments resulting in the unbalanced Fe magnetic moment in the system. Hence, the more the strain, the more is the net magnetic moment. Smaller particles show more strain than the larger one comparatively. It is to be noted that the crystallite size of BLFO (600°C) is less than that of BLFO (800°C). Strain is calculated from the FWHM of the XRD peak and the strain is proportional to the FWHM. The smaller crystallite size indicate that FWHM is more and vice versa. The crystallite size of BLFO (600°C) is less than that for BLFO (800°C) which implies that strain in BLFO (600°C) more than that of BLFO (800°C). So, the magnetization (M_r, M_s) for BLFO (600°C) is more than BLFO (800°C). It is also known that magnetization increases with decrease in crystallite size. However, the coercive field H_c for BLFO (800°C) is larger compared to BLFO (600°C) and almost it is twice as that for BLFO (600°C). Typically, H_c depends on the magnetocrystalline anisotropy (MCA) [24] which increases with increase in crystallite size. Hence, the enhanced H_c for BLFO (800°C) may be attributed to its crystallite size which greater than that for BLFO (600°C).

The magnetoelectric effect of multiferroics can be estimated from the effective magnetic susceptibility as the magnetic susceptibility χ is related to the effective dielectric constant [25]. The magnetic susceptibility is determined by the slope of the M-H curve at H=0. The magnetic susceptibility of BFO, BLFO (600°C) and BLFO (800°C) samples are given in Table 1. The χ for BLFO samples is higher than that reported by Zhang et al [26] for $Bi_{1-x}La_xFeO_3$ (x=1) samples which is 0.09 x 10^{-3} emu g^{-1} Oe^{-1}. The χ values of BLFO samples are more than that of BFO. The magnetic susceptibility of the doped samples is observed to increase with calcination temperature and it implies that that the magnetoelectric (ME) effect also increases. This argument reveals that ME interaction for BLFO (800°C) is more than that of BLFO (600°C).

3.3. Dielectric property

The measured room temperature dielectric constant as a function of frequency in the range from 50 Hz to 10 MHz is depicted in Fig. 4 for all the samples. The inset shows the variation from 100 Hz to 10 MHz. The dielectric constant for all the samples shows the same trend with variation in frequency. At very low frequency from 50 to 100 Hz, the dielectric constant decreases abruptly and it is independent in high frequency region. This is a normal behavior of dielectrics or ferroelectrics [27, 28]. At low frequency region, all the electronic and space charge polarization process can follow the change of external field resulting in high dielectric constant. However, with increase in frequency except the electronic polarization, space-charge polarization gradually gets suppressed as they do not respond to high frequency. So the contribution in the high frequency region mainly comes from electronic polarization and as a result, the dielectric constant remains unchanged in the high frequency region i.e., at low frequencies dielectric relaxation occurs. The dielectric constant (Є) at 50 Hz for BLFO calcined at 800°C (Є=$2.7x10^3$) is more than that of BLFO calcined at 600°C (Є= $0.47x10^3$) and this may be attributed to its greater crystallite size (93 nm) compared to that of BLFO (600°C) [19].

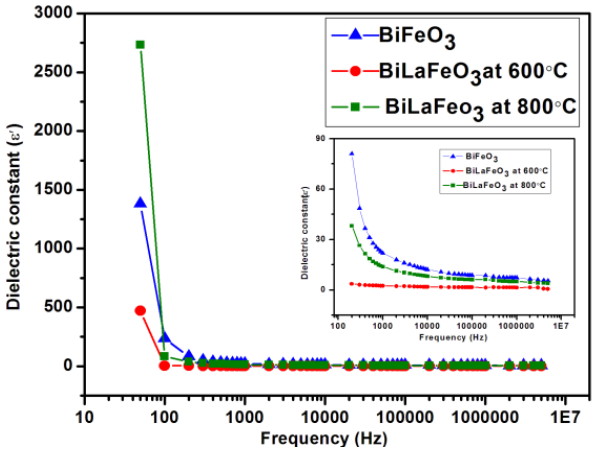

Fig. 4. Dielectric constant of pure and La doped BiFeO3

The dielectric loss versus frequency plots are given in Fig. 5 for the measured range from 50Hz to 10 MHz at room temperature. The inset presents the variation of loss tangent from 100 Hz to 10 MHz. From this, it is clear that at 50 Hz, the loss percentage for BFO is more than BLFO samples as expected. The dielectric loss is maximum in the very low frequency region and from there onwards, it drops gradually up to 100 Hz. Above 100 Hz, loss is constant and almost at zero. It is to be noted that at a low frequency of 100 Hz, the loss value for BLFO (600°C) is less than for BLFO (800°C) and this is due to its crystallite size being smaller which leads to more resistivity. In smaller size, increased grain boundary scattering leads to more resistivity and hence resulting in low loss.

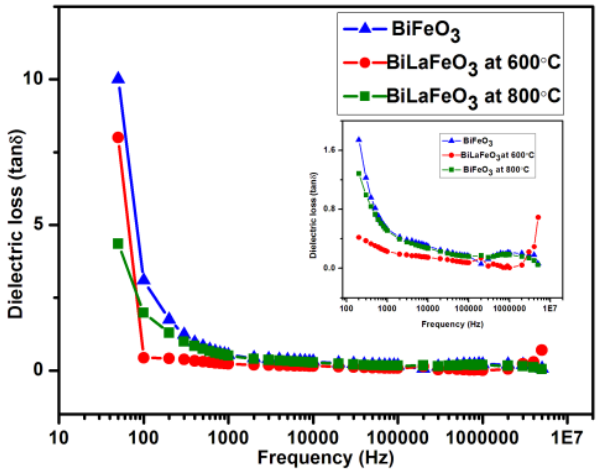

Fig. 5. Dielectric loss of pure and La doped BiFeO3

The ac conductivity σ_{ac} as a function of the measured frequency of 50 Hz to 10 MHz at room temperature is given in Fig. 6. The variation of σ_{ac} from 100 Hz to 10MHz is given in the inset. It is seen that at 50 Hz, a low conductivity of the order of $1\times10^{-5}(\Omega m)^{-1}$ is exhibited for all the samples while from 100 Hz to 100 kHz, it is almost zero. Beyond 100 kHz, it shows an abrupt rise in conductivity. In the higher frequency (> 1MHz), for BLFO, the σ_{ac} values are much less than for BFO. By and large, the very low conductivity of the BLFO samples suggest that their leakage current may be very low in the entire frequency range and probably, the nanoparticles would have caused this low conductivity [29]. However, comparatively, there is a significant difference in the values of σ_{ac} for the BLFO samples calcined at two different temperatures. Below 100 Hz and above 100 kHz, σ_{ac} is lower for BLFO (600°C) than for BLFO (800°C) sample. The low values of σ_{ac} for BLFO (600°C) can be explained as follows. As the crystallite size of the BLFO (600°C) is less than that of BLFO (800°C), this may result in the formation of smaller grain and such small grains have smaller grain boundaries leading to dense boundaries. Scattering of electron from the dense grain boundaries is more for smaller grains compared to large grains resulting in high resistivity and hence low conductivity. So, one can expect low conductivity for BLFO (600°C) compared to BLFO (800°C). In general, the low conductivity of BLFO samples also reveals their best feature of low leakage current.

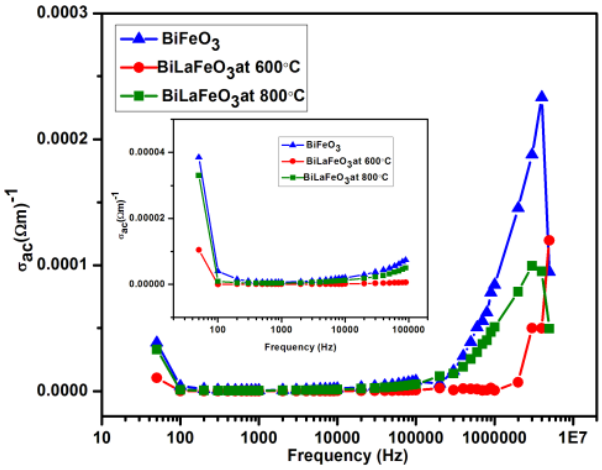

Fig. 6. Ac conductivity of pure and La doped BiFeO3

Conclusions

Pure and La doped $BiFeO_3$ nanoparticles were prepared using sol-gel method. XRD pattern confirm the formation of rhombohedral structure for all the studied samples. The average particle size of the BFO, BLFO (600°C) and BLFO (800°C) nanoparticles is 31, 56 and 93 nm respectively. The undoped BFO nanoparticles show weak ferromagnetic order at room temperature and its M_s and M_r values are lower than the doped samples. Significant saturation in the magnetic hysteresis is observed for the low calcined BLFO sample. While the highest values of M_s and M_r are observed for BLFO (600°C), the largest value of coercivity was observed for BLFO (800°C) comparatively. The dielectric constant of BLFO (800°C) is found to be more than BLFO (600°C). The ac conductivity of BLFO(800°C) is slightly more than that of BLFO (600°C) nanoparticles. Since doped samples exhibit a very low conductivity, it is expected that the leakage current should also be low. We observe low loss and low conductivity for BLFO (600°C) compared to BLFO (800°C). The magnetic susceptibility values of the doped samples demonstrate that the ME effect of BLFO (800°C) is more than that of BLFO (600°C). The present study reveals that high annealing diminishes the magnetization and also the dielectric property. Hence, a moderate annealing should be optimized meticulously for the material preparation for the multiferroic applications as the multiferroic materials are multifunctional materials.

References

1. M. Fiebig, T. Lottermoser, M. K. Kneip and M. J. Bayer, J. Appl. Phys., 99, 08E302–5 (2006).
2. N. A. Spaldin and M. Fiebig, Sci., 309, 391–2 (2005).
3. F. Yan, M. Lai, L. Lu and T. J. Zhu, J. Phys. Chem. C., 114, 6994–8 (2010).
4. Q. H. Jiang, C. W. Nan and Z. J. Shen, J. Am. Ceram. Soc., 89, 2123–7 (2006).
5. I. Sosnowska, R. Prezenioslo, P. Fischer and V. A. Murashov, J. Magn. Magn. Mater., 160, 384–385 (1996).
6. J.B. Neaton, C. Edrer, U.V. Whgmare, N.A. Splaldin and K.M. Rabe, Phys. Rev. B., 71, 014113–14118 (2005).
7. Z. X. Cheng, X. L. Wang, K. Ozawa and H. Kimura, Appl. Phys. Lett., 40, 703–713 (2007).
8. F. Zavaliche, R. R. Das, D. M. Kim, C. B. Eom, S. Y. Yang, P. Shafer and R. Ramesh, Appl. Phys. Lett., 87, 182912 (2005).
9. Z. Chang, B. Chan, X. J. Xiano, Z. H. Zao, Y. W. Zno, Y. F. Fu, Q. F. Zhan and Q. W. Li, Chins. Phys. B., 20, 11, 117701 (2011).
10. T. Zhao, A. Scholl, F. Zavaliche, K. Lee, M. Barry, A. Doran, M.P. Cruz, Y. H. Chu, C. Ederer, N. A. Spaldin, R. R. Das, D. M.Kim, S. H. Baek, B. Eom, and R. Ramesh, Nat. Mater., 5, 823 (2006).
11. X. D. Qi, J.DhO and R.Tomo, J. Appl. Phy., 86, 062903 (2005).
12. K. Kim, S. S. Kim, W. J. Kim, A.S. Bhalla and R.Guo, Appl. Phys. Lett., 88, 132901(2006).
13. F. Z. Qian, J. S. Jiang, W. G. Zhang and J. H. Liu, J.Phys. D. Appl. Phys., 43, 025403 (2010).
14. G. L.Yuan, S.W.Or, J. M. Liu and Z. G. Liu, Appl. Phys. Lett., 89, 052905 (2006).
15. S. T. Zhang, Y. Zhang, M. H. Lu, C. L. Du, Y. F. Chen, Z. G. Liu, Y. Y. Zhu and N. B. Ming, Appl. Phys. Lett., 88, 162901 (2006).

16. G. L.Yuan, S.W.Or, and H. L. W. Chan, Appl. Phys. Lett., 10, 064101 (2007).
17. Y. Qiu, Y. S. Luo, Z. J. Zox, Z. M.Tian, S. L.Yuan, Y. Xi and L. Z. Huaing, J. Mat. Sci. Mater. Electron., 25, 760-764 (2014).
18. J. Chun Zhao, Ce Zhao, Matthew Werner, Steve Taylor, Paul Chalker and Peter King, Nanoscale Res. Lett., 8,172 (2013).
19. M. Hojamberdive, Y. Xu, F. Wang, W. Liu and J. Wang, Inorg. Mater., 45, 10, 1183-1187 (2009).
20. Dimple P. Dutta, Balaji P. Mandal, Ratna Naik, Gavin Lawes and Avesh K.Tyagi, J. Phys. Chem. C, 117, 2382-2389 (2013).
21. D. C. Jia, J. H. Xu, H. Ke, W.Wang and Y. Zhou, J. Eur. Ceram. Soc., 29, 3099-3103 (2009).
22. Magne, Samar Layek and H. C. Verma, Adv. Mat. Lett. 3, 6, 533-538 (2012).
23. Pragya pandit, S. Satapathy, Poorva Sharma, P. K, Gupta, S. M. Yusuf and V.G. Sathe, Bull. Mater.Sci., 34, 4, 899-905 (2011).
24. F. Huang, X. Lu, W. Lin, X.Wx, Y. Kan and J. Zhu, Appl. Phys. Lett., 89, 242914 (2006).
25. N . Wang, J . Cheng, A. Pyatakov, A. K. Zvezdin, J. F. Li, L.E. Cross and D. Viehland, Phys. Rev. B., 72, 104434 (2005).
26. Shan Tao Zhang, Ling Huna Pang, Yi Zhang, Ming Hiu Lu and Yan Feng, J. Appl. Phys., 100, 114108 (2006).
27. Y. Qiu, Y. S. Luo, Z. J. Zox, Z. M. Tian, S. L. Yuan, Y. Xi, L. Z. Huaing, J. Mat. Sci. Mater. Electron., 25, 760-764 (2014).
28. M. Idrees, M. Nadeem, M. Atif, M. Siddique, M. Mehmood and M. M. Hassan, Acta Mater., 59, 1338 (2011).
29. Gagan kumar, Sucheta sharma, R .K. Kotnala, Jyoti Shah, Sagar E.Shirsath, Kalid M. Batoo and M.Singh, J. Mol. Struture, 1051, 336-344 (2013).

*****